JOURNAL OF CATALYSIS 126, 572–590 (1990)

Low-Temperature Thermal and Photoactivation of TiO_2-Supported Ru, Rh, and Cu Catalysts for CO–NO Reaction

K. RAVINDRANATHAN THAMPI,[1] P. RUTERANA,* AND M. GRÄTZEL

*Institut de Chimie Physique and *Institut Interdepartemental de Microscopie Electronique, Ecole Polytechnique Fédérale de Lausanne, CH-1015, Lausanne, Switzerland*

Received February 12, 1990; revised June 15, 1990

TiO_2 (P25)-supported Ru catalysts are active for NO–CO reaction at temperatures as low as ambient in a batch reactor. Reaction products are CO_2, N_2O, and N_2. In a fixed-bed reactor, this reaction was monitored from 90 to 235°C. The activity increased exponentially above 150°C. On illumination with light energy ($\lambda \leq 390$ nm), the rate of decomposition of N_2O, a product formed during the reaction, is enhanced significantly. N_2O has been shown to react with CO as well. All photoactivation experiments have been performed in batch reactors. Photoprocesses are support related and a reaction mechanism has been put forth to explain the observed phenomena. The catalyst prepared by the deposition–precipitation technique shows selective dispersion of Ru particles over the rutile phase of TiO_2 from a mixture of 80% anatase and 20% rutile (composition of P25). Addition of Rh and Cu increases the N_2O decomposition property of the catalyst.

1. INTRODUCTION

In addition to automobile exhausts, stationary installations such as power plants and industrial stacks are major sources of CO and NO_x emission. Processes that are commercially available have been developed, particularly in Japan and in The Netherlands (*1*). At present, this technology is expensive and hence not suitable for wider applications (*1*). Other limitations to the system include (i) elevated operating temperatures and (ii) use of NH_3 as a reductant of NO_x, causing NH_3 emission unless processed again to remove the unreacted NH_3 (*1, 2*). Therefore, it is desirable to design a new process which is more acceptable for practical use.

In this paper we present our results on the reaction between CO and NO on a few supported Ru, Rh, Cu, Ru–Rh, and Ru–Cu catalysts. In addition to thermal activation, it was our aim to make these catalysts light sensitive in order to enhance catalytic activity at low temperatures. Such catalytic systems could ultimately lead to the design of a photothermally activated, environmentally clean, low-cost technology for NO–CO removal from stationary sources. Since these systems are thermally active, they can also be operated without light, when it is required (*3*). To our knowledge, photocatalytically activated CO oxidation using NO has not been reported earlier. Photocatalytic oxidation of CO on oxides such as TiO_2, ZrO_2, SnO_2, WO_3, and SiO_2 has been studied by Lyashenko and Gorokhovatskii (*4*) using a static system. A photoenhancement on the rate of photooxidation of CO by O_2 over Pd when the total pressure of the system was about 20 torr has been reported (*5*). At low pressures no such photoenhancement was visible and the actual mechanism is not well understood. There are also reports on the photodesorption of CO from Ni (*6*).

The catalytic reduction of NO_x to N_2, N_2O, and NH_3 by CO, hydrocarbons, and H_2 has been studied widely (e.g., Refs. (7–9)). Hardee and Hightower have used CH_4 as a reducing agent for NO over Rh/

[1] To whom correspondence should be addressed.

0021-9517/90 $3.00

Al_2O_3 catalysts (*10*). Steady-state kinetics of the catalytic reduction of NO_2 by CO have been reported (*11*). Oxidation of CO with NO and O_2 is also a rigorously studied topic (*12, 13*). Pt, Pd, Rh, Ru, Cu, etc., were termed the most active metals (especially in the realm of three-way automobile exhaust catalysts) when supports such as SiO_2, Al_2O_3, ZrO_2, La_2O_3, and CeO_2 were employed (*14*). Apart from metal-supported catalysts, several other substances, such as perovskites, have been tried in these reactions (*15*). Reduction of NO by CO has been achieved using homogeneous catalysts of Rh, Co, Ir, Ru, Fe, Os, Cu, and Pd complexes and salts (e.g., Refs. (*16, 17*)) in solution.

We have selected Ru, Ru–Rh, and Ru–Cu loaded catalyst for our initial investigations. Compared to other metals, Ru shows a high specificity for the reduction of NO to N_2 rather than to NH_3 (*14*) (for feeds containing H_2), in addition to its activity for CO oxidation (*18*). Over Rh catalysts, NO is reduced to N_2 rather than to NH_3, provided that the reactor is not operating under net-reducing conditions (*14*). Also, as an oxidation catalyst for CO, Rh has a favorable specificity and activity at low temperatures (*14*). A $Ru–RuO_x/TiO_2$ catalyst is light sensitive for several photoinduced and thermally activated reactions (*19, 20*). For the reduction of NO by CO, the activity sequence is Ru > Rh > Pt > Pd (*21*). However, Ru catalysts have been studied for NO–CO reaction less frequently, and relatively few reports on this metal are available (*7, 14, 22*). This is because Ru is unstable owing to the formation of volatile oxides, RuO_3 and RuO_4. However, when the catalyst is photothermally activated, such problems are minimal because the reaction temperature is not meant to be far above ambient. Over a range of catalysts with only a few exceptions, the $CO–O_2$ reaction rate has been found to be faster than that of CO–NO (*23*). Therefore, in the present study to avoid complexities, only CO and NO were used as the reactants along with He diluent. Reactions were carried out on a reduced catalyst to limit the number of parameters at this stage, although some catalysts for this reaction have been shown to be more active when they were preoxidized (*24*). Because one of the products was N_2O, we tried to study a few Cu-supported catalysts as well. Cu and its oxide were reported to be fairly active for N_2O decomposition (*25, 26*). Likewise Cu-containing cuprates and perovskites are well known for N_2O decomposition (*27*) as well as CO oxidation (*28*). TiO_2 was used as the main catalyst support for the following reasons:

(1) TiO_2 absorbs light $\lambda \leq 410$ nm and causes excitation of electrons from valence band to conduction band enabling the catalyst to be photoactive.

(2) TiO_2 is SO_x resistant to some extent (*29*).

(3) Electron transfer to TiO_2 is possible, thereby enabling the enhancement of catalytic activity.

(4) The catalytic reaction may be influenced by taking advantage of metal support interaction, for which TiO_2 is the most suitable support material.

2. EXPERIMENTAL

Catalysts consisting of Ru, Rh, Cu, Ru–Rh, or Ru–Cu supported on TiO_2 (P25, Degussa; BET area 55 m^2/g), Al_2O_3 (C, Degussa; BET area 100 m^2/g), and SiO_2 (aerosil, Degussa; BET area 90 m^2/g) were prepared as their corresponding oxides via deposition–precipitation, using a procedure previously reported from this laboratory (*19, 20*). The pH of the deposition step was varied according to the nature of metal. Required amounts of $RuCl_3 \cdot$ hydrate (Fluka), $RhCl_3 \cdot$ hydrate (Fluka), and $CuCl_2$ (Fluka) were dissolved in 150 ml 0.1 *M* HCl. The support was added to the solution and it was warmed to 70°C with constant stirring. NaOH at 0.1 *M* was added slowly over 6–7 h to raise the pH of the suspension to the required level at 70°C. For Ru the pH was 4, while for Rh and Ru–Rh it was 8.7.

For Cu and Ru–Cu the neutralization was stopped at pH 8.5. The suspension was then allowed to evaporate to dryness at 90°C. This powder was then heated to 170°C for 18 h followed by 370°C for another 18 h in air. Residual Cl^- and Na^+ ions were eliminated by dialyzing the powder for 4 days. After dialysis the catalyst was dried and stored. Elemental analyses of the finished catalyst samples were carried out to determine the level of impurities and the results are as follows: C = 0.1%, Cl^- = 0.06 ± 0.01%, Na^+ = 84 ± 8 μg/g, and K^+ = 25 ± 5 μg/g.

Thermally activated catalytic reactions were carried out using a fixed-bed reactor. The U-type reactor was made of Pyrex or quartz and the catalyst was fixed into position using plugs of glass wool. The temperature of the catalyst bed was controlled by a well-type furnace equipped with an electronic controller and a thermocouple. All gas flows were measured through precalibrated rotameters before entering the reactor. Pure gases and gas mixtures such as 25% CO or 15% NO in He were supplied by Carbagas Company of Switzerland. Gas mixtures were used without further purification. Ar, He, and H_2 were purified by an oxisorb column to remove traces of O_2. Analysis was carried out using a gas chromatograph equipped with a thermal conductivity detector. For analyzing CO and N_2 a molecular sieve 5 Å column and for CO_2, N_2O, and NO a Porapak QS column were used. The carrer gas was He.

Before the catalytic run, the catalysts were pretreated in the following manner. For all experiments 100 mg catalyst (5% $RuO_2/TiO_2 \equiv 3.8\%$ Ru/TiO_2) was used. First it was reduced at 230°C for 1 h in a current of 1 : 1 He and H_2 (40 ml/min total flow). In this way the catalyst was reduced partially to obtain a working catalyst of the form $Ru–RuO_x/TiO_2$ (*19, 20*). To remove the excess H_2 after reduction, the catalyst was kept in a stream of He for another 2 h at the same temperature. Subsequently, the reactor was brought down to the reaction temperature and the He flow was maintained for another 18–20 h. Before the reacting gases were let in, an analysis was carried out to confirm the absence of H_2 in the flowing gas stream. After each set of experimental runs in a given feed composition, the catalyst was again treated in a stream of He at 230°C for 5–7 h before testing with a different gas composition. Since the run lasted several days, a flow of He was maintained in the reactor when there were no reactants present.

Photochemical activation was accomplished using a cell described previously (*19, 20*). Catalyst (100 mg) was spread over the bottom of a flat Pyrex cell (volume 20–24 ml) equipped with side arms and septum for admission and withdrawal of gas samples. Our earlier photocatalytic studies at ambient temperature and pressure using this batch reactor provided valuable results when the reactions studied were sufficiently slow. Under mild conditions, the use of a flow reactor would not be helpful when the reaction yields are poor. The results obtained with our batch reactor were complimentary to the data obtained with a recirculation reactor attached to a diffuse reflectance FT-IR system (*30, 31*). No mass or heat transfer effects were noted under the present experimental conditions. The volume and size of the batch reactor were varied by about 20% and no variations in the kinetic data were observed. The catalyst was pretreated in a manner similar to that described in the previous paragraph. After treatment the cell was isolated and the required gas mixtures were injected. The cell was illuminated in a solar simulator (Hanau, Suntest) with a total output of 80 mW/cm^2. The sample platform was cooled by a fan. The temperature of the catalyst particles was measured by a fine-probe Ni–Cr/Ni thermocouple (Cole Parmer). These temperature recordings were compared with those obtained by an infrared image camera (Inframetrics 525), which was operated at level 55 for a temperature range up to 100°C. The cooling medium was liquid nitrogen. Trans-

mission electron microscopy (TEM) was carried out in a Philips EM 430 ST microscope, which has a point resolution better than 2 Å. Samples were suspended in ethyl alcohol to be spread on holey carbon-coated Cu grids just before observation. EELS (electron energy loss spectra) were acquired on a VG HB5 STEM microscope, which provides an electron beam diameter smaller than 1 nm.

3. RESULTS AND ANALYSIS

3.1. Physical Properties of the Catalyst

Catalysts prepared by impregnation and exchange methods have been studied rigorously for a variety of reactions including CO + NO (*1, 2, 12, 22, 24, 26*). Recently, we have shown that TiO_2-supported Ru catalysts prepared by a deposition–precipitation technique have, in addition to their low-temperature catalytic activation abilities, interesting surface morphology (*32*). In this paper we examine this aspect only briefly. TEM studies on a catalyst prepared in this way show that only a selected number of TiO_2 crystallites were covered with Ru (Fig. 1). The support material, i.e., TiO_2(P25), contains 70–80% anatase and 20–30% rutile. The uneven distribution was not observed for catalysts prepared in a similar manner with other metals such as Rh, Pt, Co, and Ni. It was not observed even for other forms of TiO_2 like pure rutile or anatase. The selectively dispersed RuO_x particles were examined under the high-resolution microscope, and the largest among them was identified as RuO_2 from their 100 lattice fringes (*32*). Although encountered on a fresh catalyst as well, the selective dispersion is much more clearly visible on a catalyst used for reactions for a long time (spent catalysts) or on a fresh catalyst reduced in H_2 at 500°C for 1 h. With such treatments the noble metal particles were sintered partially. The support crystallites also appear to have a morphology highly different from that of the nonloaded ones. However, unlike spent catalysts, the samples after H_2 reduction at 500°C showed larger Ru particles exclusively made of metallic Ru, as evidenced by its 101 lattice fringes. We have used EELS to establish the structure of TiO_2 particles on which RuO_x was selectively deposited. Figure 2a shows the EELS taken on TiO_2 crystallites not loaded with RuO_x. It is in agreement with the spectrum of pure anatase (shown as inset). Figure 2b shows the corresponding spectrum for selectively loaded TiO_2 particles. This is in good agreement with the spectrum of pure rutile (see inset).

3.2. Thermal Activation

First it was necessary to check the activity of the finished catalyst under thermal activation. A mixture of NO and CO in He was passed over the pretreated catalyst at the rate of 5 ml/min, and the reactor temperature was 89°C. The composition of the reactant gas mixture was 7.5% NO, 12.5% CO, and 80% He. Reaction products were CO_2, N_2O, and N_2. Traces of H_2O and CH_4 that also appeared at the beginning of the reaction originated from residual H_2 bound strongly on Ru/TiO_2 during the reduction stage. After several minutes they disappeared from the product stream. At the start of the reaction the catalytic activity was relatively high but slowed down to a steady-state level with time. Depending on the reaction temperature, this time varied from 1 to several hours. Figure 3 shows the conversion level of N_2O, CO_2, and N_2 at steady state as a function of reaction temperature. Percentages of NO and CO converted as N_2O and CO_2 were calculated as follows:

$$\%\ \text{CO converted as } CO_2 = \frac{\text{amount of } CO_2\text{/ml in product stream}}{\text{amount of CO/ml in reactant mixture}} \times 100$$

$$\%\ \text{NO converted as } N_2O = \frac{\text{amount of } N_2O\text{/ml in product stream}}{\text{amount of NO/ml in reactant mixture}} \times 200$$

In this calculation it is assumed that all the

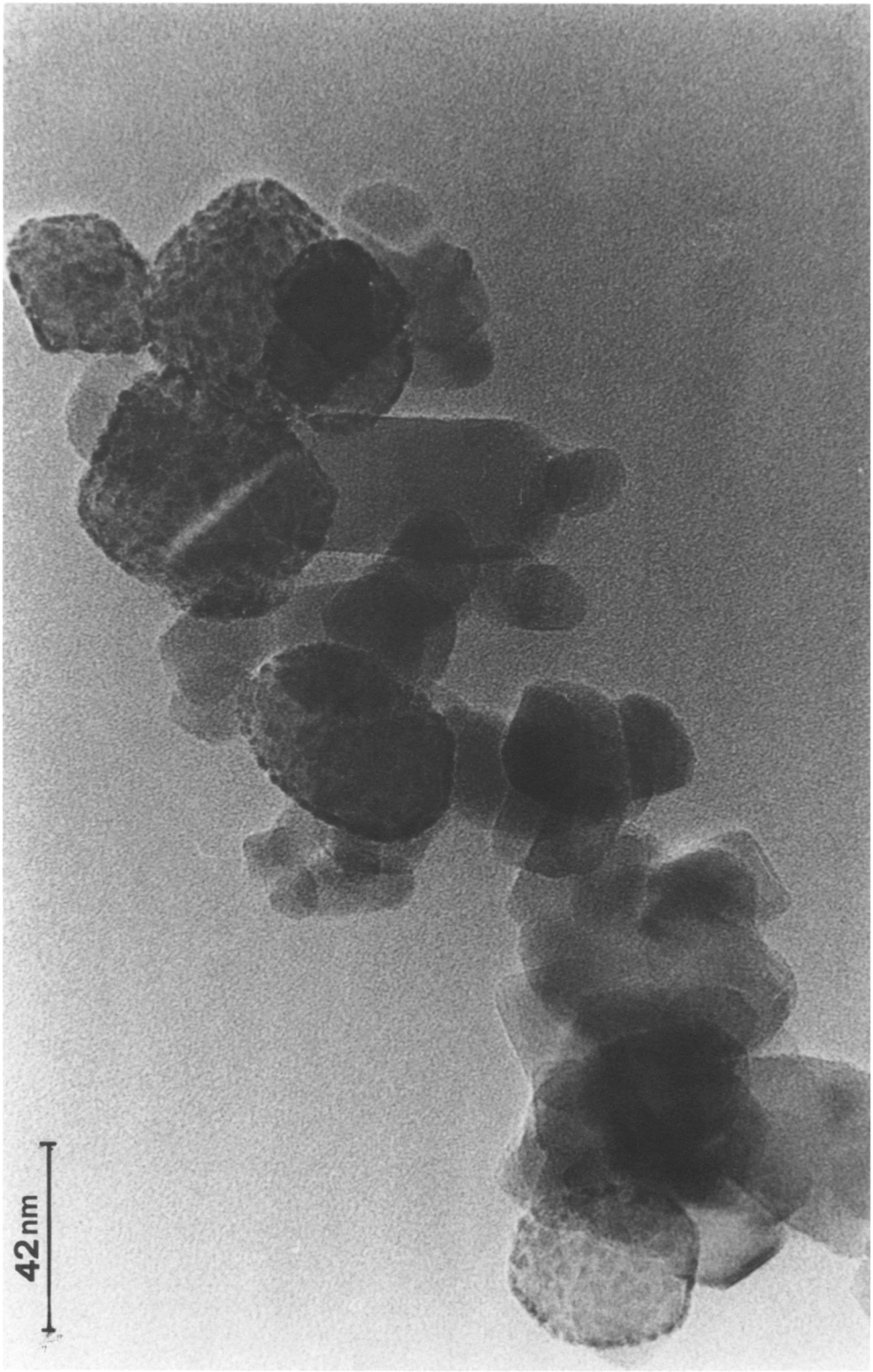

FIG. 1. TEM showing distribution of ruthenium oxide on selected TiO_2 crystallites.

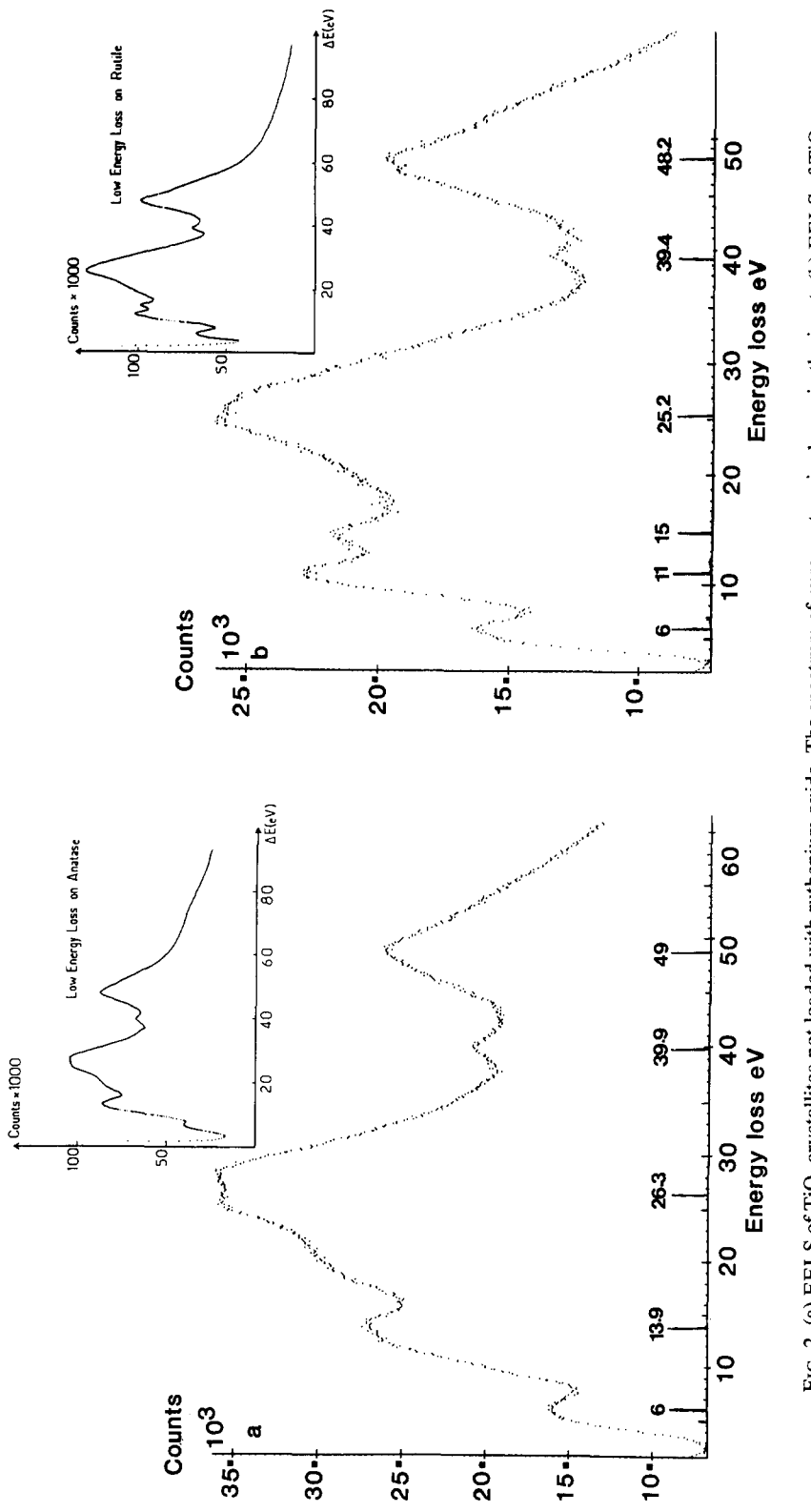

FIG. 2. (a) EELS of TiO_2 crystallites not loaded with ruthenium oxide. The spectrum of pure anatase is shown in the inset. (b) EELS of TiO_2 crystallites loaded with ruthenium oxide. The spectrum of pure rutile is shown as inset.

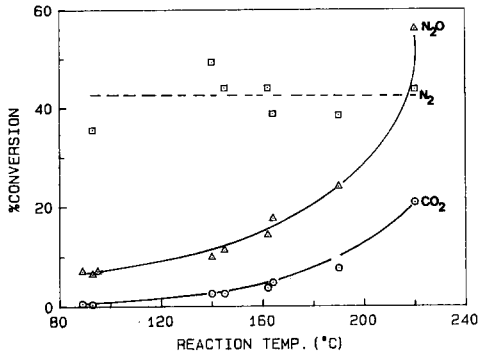

FIG. 3. Conversion of NO to N_2O/N_2 and CO to CO_2 as a function of temperature when CO and NO were reacted together over 100 mg 3.8% Ru/TiO_2 catalyst in a flow reactor.

CO_2 produced is via the CO + NO reaction or the CO + $O_{(s)}$ reaction, where $O_{(s)}$ is from the surface of the partially reduced catalyst.

Typical values for the conversion of NO and CO are as follows: at 90°C, percentage NO converted to N_2O was 7.1 and percentage CO converted to CO_2 was 0.6. Taking into account the amount of N_2 (7.5% NO, 1 ml of $N_2 \equiv 2$ mol of NO) in the product, the total conversion of NO at 90°C was calculated as 42.6%. The percentage NO converted to N_2 did not vary significantly with the increase in temperature. This value was always within 35–53% and centered around 39–44% in most of the runs. The conversion to N_2O increased to 11.3% for NO and 2.6% for CO to CO_2 at 145°C. At 220°C the percentage CO converted to CO_2 was 20.8% while that of NO conversion to N_2O was 56%. The value for NO to N_2 remained at 43.7%. The total conversion of NO is therefore 99.7%.

In separate experiments pure CO or NO was passed over the catalyst along with He. The reacting gas mixture contained 7.5% NO or 12.5% CO and the remaining He. The total flow was maintained at 5 ml/min. Percentages of NO converted to N_2O/N_2 and CO converted to CO_2 are shown in Fig. 4 as a function of temperature. Results indicated that when NO alone was passed through the catalyst, the amounts of N_2 and N_2O did not vary significantly with temperature. The percentage of NO converted to N_2O remained 5.4–6% throughout the temperature range 93–255°C. The percentage of NO converted to N_2 remained between 35 and 41 in this temperature range.

The dispersion of Ru in 3.8% Ru/TiO_2 determined by the H_2 adsorption technique was 28.2%, assuming a 1 : 1 stoichiometry for the chemisorption of H by surface Ru.

3.3. Photothermal Activation of NO and CO

3.3.1. Temperature measurements on an illuminated particle. It is important to determine the temperature of the catalyst particles under illumination before proceeding further with the photochemical activation. It is a difficult task to determine the exact temperature of a catalyst particle under light irradiation and an analysis of this problem is available in the literature (*33*). We have used a fine-probe thermocouple and an infrared image camera to establish the particle temperature distribution. The highest temperature recorded by the thermocouple was 52°C and the lowest was 40°C. The infrared camera recorded the highest particle temperature to be between 55 and 57°C. Since the relative number of these high-temperature particles was low, the mean tempera-

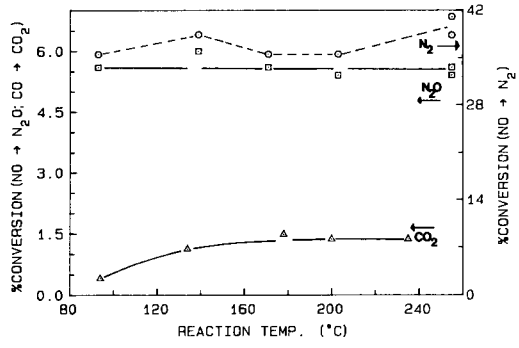

FIG. 4. Conversion of NO to N_2O/N_2 and CO to CO_2 as a function of temperature when pure CO or NO was passed through 100 mg 3.8% Ru/TiO_2 catalyst in a flow reactor.

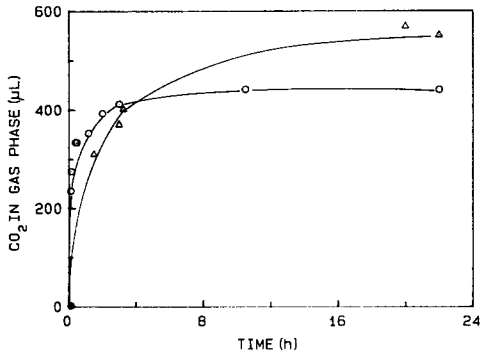

FIG. 5. CO_2 in gas phase as a function of time when 1 ml CO was reacted over 100 mg 3.8% Ru/TiO_2 catalyst with (△) and without (⊙) illumination.

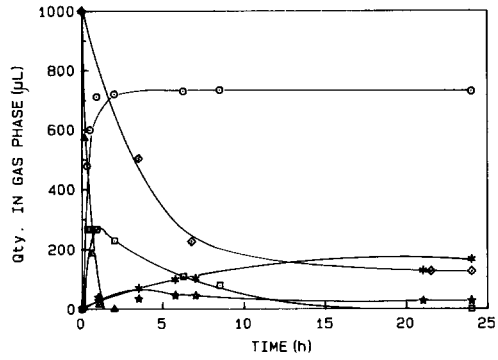

FIG. 6. CO, CO_2, and N_2O as a function of time of illumination. 1 ml CO and 815 μl NO were initially injected. (a) 100 mg 3.8% Ru/TiO_2: ⊙, CO_2; △, CO; and ⊡, N_2O; (b) 100 mg TiO_2 (P25): *, CO_2; ◇, CO; and ★, N_2O.

ture of the catalyst bed was taken to be that measured by the thermocouple (52°C). Separate photocatalytic experiments were carried out at 57°C and still the contribution from light energy was significant.

3.3.2. Catalytic experiments in batch reactors. Figure 5 shows CO_2 formed and desorbed to gas phase as a function of time when 1 ml CO was allowed to oxidize/disporportionate over 100 mg 3.8% Ru/TiO_2 catalyst at 52°C with and without UV illumination. The reproducibility of kinetic data was better than ±3%. When 1 ml CO and 815 μl NO were injected over 100 mg 3.8% Ru/TiO_2 and pure TiO_2 (P25), the products were CO_2, N_2O, and N_2. Figure 6 shows the plot of CO, CO_2, and N_2O as a function of illumination time. The degree of reaction on pure support is also indicated in Fig. 6 for comparison. For reasons of clarity, the plot for NO consumption and N_2 production is not shown. The disappearance of NO should correspond to the equivalent sum of N_2O and N_2 in the system. However, it was not possible to check this because of the strong adsorption of NO on the catalyst under the experimental conditions. Chromatographic analysis could only give the composition of gas phase. This reaction, if carried out in dark at the same temperature (52°C), would behave differently (Fig. 7). This shows that most of the nitrogen atoms are still present as N_2O. However, when the catalyst was contacted with 1 ml CO and 370 μl N_2O (N_2O is on the same order as that remaining after 24 h in Fig. 7), the levels of reaction under dark and illumination were more or less identical. All the N_2O was consumed at the end of 8 h with concomitant formation of CO_2. In separate experiments when 1 ml N_2O was contacted with 200 mg Ru/TiO_2 catalyst, in little over 3 h under illumination all the N_2O disappeared from the gas phase. Even after 18 h, when the same experiment was conducted in dark, small amounts of

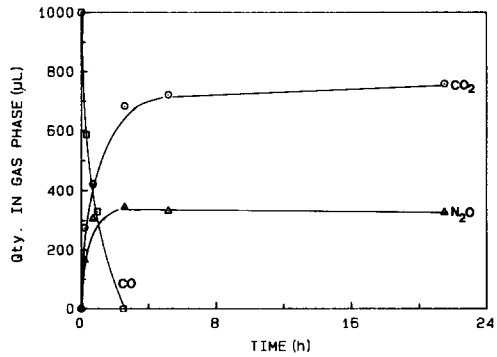

FIG. 7. CO, CO_2, and N_2O as a function of time in dark. Other details are similar to those in Fig. 6.

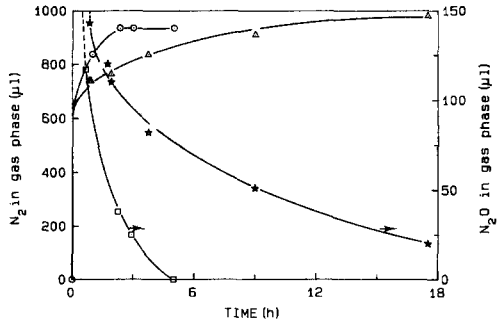

FIG. 8. One milliliter of N_2O over 200 mg of 3.8% Ru/TiO_2 catalyst: (a) Under illumination: ⊙, N_2; ⊡, N_2O; and (b) in dark: △, N_2; ★, N_2O.

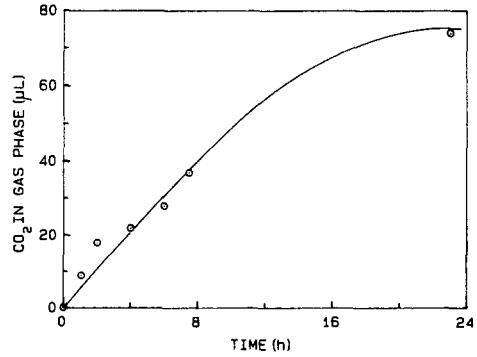

FIG. 10. Production of CO_2 from CO on 100 mg 3.8% Ru/SiO_2 in dark. One milliliter of CO initially injected.

N_2O remained in the cell (Fig. 8). This shows that N_2O could react with CO and the reaction rate is not influenced by light. However, in the absence of CO, N_2O decomposition is aided by light. Figure 9 shows the effect of TiO_2 support on N_2O decomposition when this reaction was carried out with and without light irradiation. The level of CO oxidation/disproportionation on SiO_2-supported Ru catalysts is low even after 24 h of reaction. A comparison of Figs. 5 and 10 reveals this fact. This observation is valid for a reacting gas mixture containing CO and NO as well. SiO_2 is not photosensitive, while Al_2O_3 could exhibit small photo responses to UV radiations depending on the experimental conditions. It is attributed mostly to surface-state energy levels located in the band gap region of Al_2O_3 (*34, 35*). Figure 11 shows a plot of N_2O, CO, and CO_2 as a function of time when 3.8% Ru supported on Al_2O_3 and SiO_2 are irradiated in the presence of 1 ml CO and 850 µl NO at 52°C. Even after 24 h, the N_2O remained in gas phase without full reduction.

In the course of our study we have noticed that H_2, if present in the system, could retard the CO + NO reaction and N_2O decomposition (Fig. 12). In such circumstances CO_2 is methanated to CH_4, confirming the presence of other parallel reactions. This is understandable because this catalyst was shown to exhibit room temperature metha-

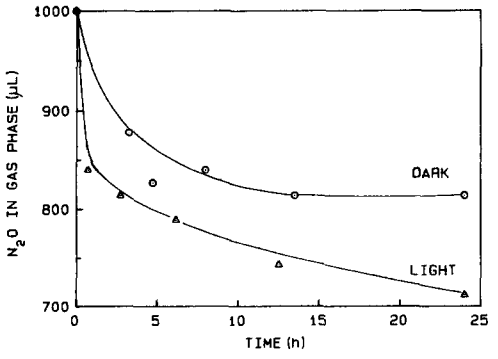

FIG. 9. Effect of TiO_2 (P25) support on N_2O decomposition in dark and under illumination.

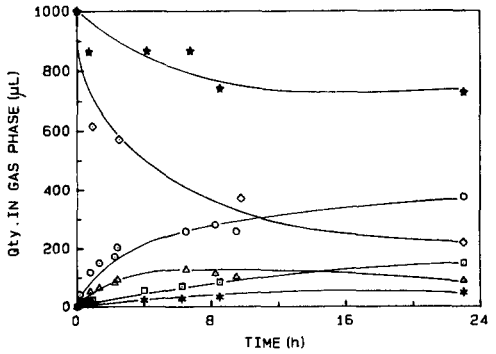

FIG. 11. One milliliter of CO and 850 µl of NO over (i) 3.8% Ru/Al_2O_3: ⊙, CO_2; △, N_2O; ◇, CO; and (ii) 3.8% Ru/SiO_2: ⊡, CO_2; *, N_2O; ★, CO (experiment under light).

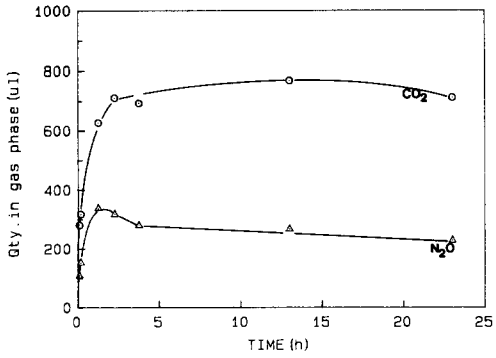

FIG. 12. Influence of H_2 on CO–NO reaction and N_2O decomposition (catalyst: 100 mg 3.8% Ru/TiO_2; reactants: 815 μl NO + 1 ml CO + 100 μl H_2).

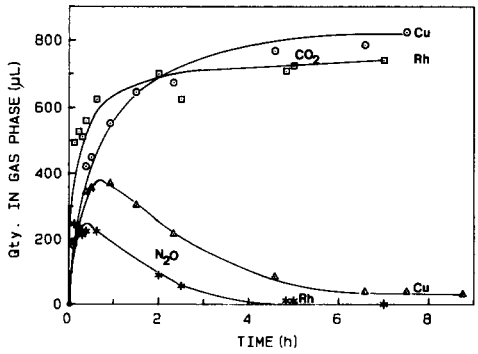

FIG. 13. N_2O and CO_2 produced as a function of illumination time for 100 mg of 3.8% Cu or Rh supported on TiO_2. One milliliter of CO and 815 μl of NO were used as reactants.

nation (*19, 20*). The rates of such reactions have been shown to be enhanced by photoirradiation (*19, 20*). Previous studies have shown that when the reacting gases are CO, NO, and H_2, Ru catalysts have a marked preference for CO + NO reaction over CO or NO reduction by H_2 (*7*). Kobylinski and Taylor (*7*) have reported that for Ru catalysts the reaction rate is relatively lower for Eq. (1) compared to that of NO–CO.

$$2NO + 5H_2 \rightarrow 2NH_3 + 2H_2O. \quad (1)$$

Furthermore, H_2O formed as a by-product during NO + H_2 or methanation reaction passivates the catalyst's active surface (*7, 19, 30, 31, 36*). In fact, it has been proved that under such conditions, water–gas shift and reverse shift reactions,

$$CO_2 + H_2 \leftrightarrow CO + H_2O, \quad (2)$$

take the lead in deciding the fate of several other reactions (*30, 31*). CO oxidation is thus retarded. Probably the sites that are active for N_2O decomposition are no longer accessible to the N_2O molecule because of the competition from other molecules such as CO_2, H_2, and H_2O and to a lesser extent CO and CH_4. Since N_2O decomposition is a slow reaction compared to CO oxidation, unreacted CO in the system can definitely block a few sites from N_2O.

3.3.3. Effect of addition of Cu and Rh. The next part of this study deals with the influence of the addition of other metals to the working catalyst. This was done mainly to influence the N_2O decomposition property of the catalyst. Figure 13 represents the photocatalytic activity of 3.8% Rh/TiO_2 and 3.8% Cu/TiO_2 catalyst for NO + CO reaction at 52°C. A combination of Ru and Rh or Ru and Cu supported on TiO_2 was shown to be much more active than the respective individual elements in supported form. (The reactivity of 7.6% Ru/TiO_2 was inferior to that of 3.8% (Ru + Rh)/TiO_2.) The data are presented in Fig. 14.

3.4. Analysis of CO Oxidation Data

From the results presented so far it is clear that partially oxidized Ru supported on TiO_2

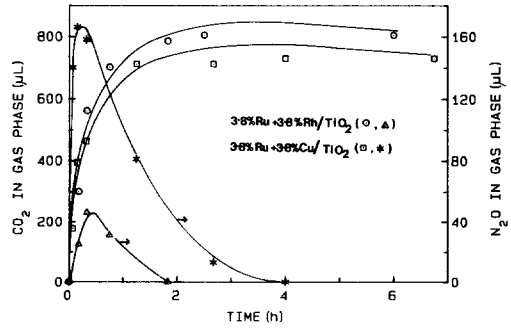

FIG. 14. CO_2 and N_2O as a function of illumination time for 100 mg catalyst.

is capable of oxidizing CO to CO_2 without added O_2 in the system even at room temperature. This leads to several possibilities: (i) CO is disproportionated to CO_2 by the well-known Boudouard reaction,

$$2CO \rightarrow CO_2 + C; \quad (3)$$

(ii) CO is reacting with oxygen from the catalyst surface, i.e., from Ru–RuO_x species causing a net reduction of the catalyst surface; and (iii) H_2O leftover from the initial catalyst reduction step remains strongly adsorbed on the catalyst surface because of the hydroxylated nature of TiO_2 support. This water interferes in the sequence because water–gas shift reaction is thermodynamically downhill. Because the H_2 produced is a small quantity it could remain chemisorbed on the catalyst until it is further reacted. In fact, our earlier studies on this catalyst by means of gas adsorption techniques and diffuse reflectance infrared Fourier transform (DRIFT) spectroscopy (*20, 36*) have proved a strong coadsorption synergy between H_2 and CO_2 with extensive hydrogen spillover. When CO_2 and H_2 are present on the catalyst, a reverse shift reaction proceeds, accumulating CO on the metal site. On mild heating, this CO was shown to undergo Boudourd reaction readily (*36*). These observations underline the necessity of identifying the major CO oxidation pathway. The following experiments were carried out to obtain this information.

3.5. CO Oxidation Pathways

Three hundred milligrams of 3.8% Ru/TiO_2 catalyst was reduced in a current of 1 : 1 moisture-free H_2 and He at 225°C for 1 h. After cooling of the sample in flowing He to the ambient, the reactor was evacuated to a pressure of 10^{-6} torr (1 torr = 133.3 N m^{-2}). Subsequentially the catalyst was heated to 300°C for 2 h at a pressure of 10^{-7} torr. After the catalyst cooled to room temperature, moisture-free He was admitted into the cell along with 1.5 ml pure CO to arrive at atmospheric pressure; 1.5 ml CO corresponds to two monolayers if we take into account the 28.2% metal dispersion and one CO for one exposed Ru. The amount of CO_2 produced over the catalyst was measured as a function of time at 24°C in dark. After 7 min 45 μl CO_2 was found in the gas phase, while after 7 h this quantity was about 215 μl. In 31 h a total of 415 μl CO_2 was noted in the gas phase. It is also important to note that the rate of CO_2 production from CO + NO reaction is significantly higher than that observed when CO was allowed to react without other added reactants. However, it is not possible to rule out the total lack of participation of oxygen from Ru–RuO_x species. Only isotopic labeling can clearly reveal this aspect and we have not attempted that in the present study. After the experiment the catalyst was further investigated using transmission electron microscopy. CO disproportionation according to Eq. (3) should leave behind nongraphitic carbon residues on the catalyst surface. Figure 15a is a TEM micrograph showing amorphous overlayers believed to have come from the CO disproportionation reaction. Figure 15b represents catalyst particles that are free of such overlayers. Further evidence for the deposition of the surface carbon was gained through the following experiment. The catalyst after the experiment was evacuated to 10^{-2} torr at 105°C for 2 h. At this temperature the deposited carbon would not become graphite and hence should become reduced to CH_4 in an H_2 atmosphere. Therefore a mixture of Ar and H_2 was introduced at 60°C, and within a short time CH_4 began to appear in gas phase. A trace of CO_2 also appeared during the very first analysis.

When 100 mg catalyst was contacted with 1 ml CO in the presence of water vapor, the formation of CO_2 was instantaneous. In less than 2 min 240 μl CO_2 appeared in the gas phase. The reaction rate slowed down after 15 min and after 4.5 h only 460 μl CO_2 was accumulated. All the CO disappeared from the gas phase. From separate experiments we noted that CO_2 adsorption in this catalyst

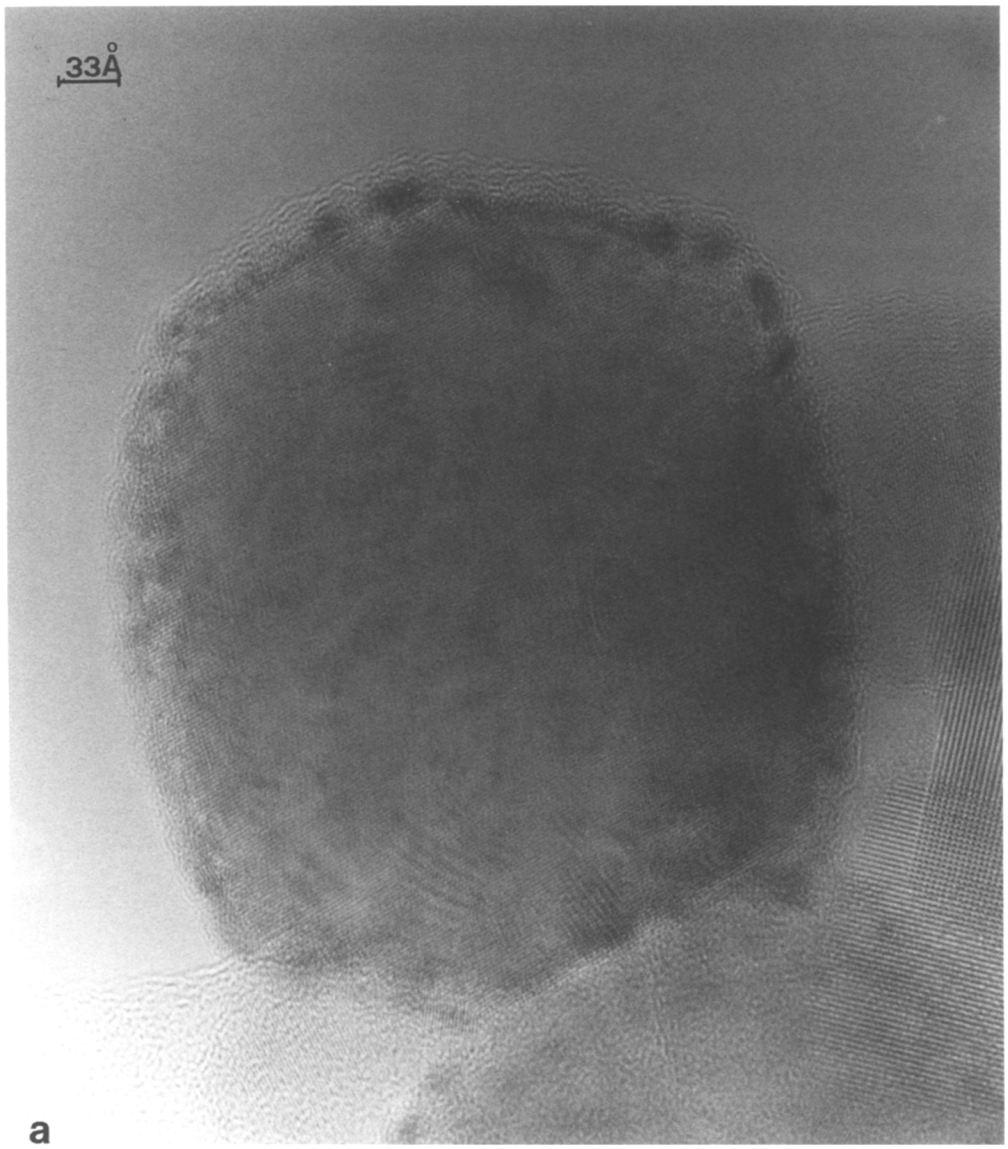

FIG. 15. (a) TEM showing overlayers of light material;

is significant. When 1 ml CO_2 was contacted with 100 mg catalyst, approximately 350 μl CO_2 remained adsorbed.

4. DISCUSSION

4.1. Catalyst Morphology

This study not only deals with a conventional heterogeneous catalytic reaction, but also is an attempt to activate the reaction under mild conditions with or without the help of illumination. Therefore it is essential to understand the catalyst from both a physical and a chemical point of view. The absorption of light is very much dependent upon the surface morphology of the material. Indeed the selective distribution of Ru on rutile phase is an interesting observation.

FIG. 15. (b) TEM showing similar catalyst particles without overlayers.

Presumably this happened because of the difference in the surface free energy of rutile and anatase phases of TiO_2. A correlation exists between the ion-exchange capacity and the net surface charge carried by the hydrated oxide (*37*). The isoelectric points (iep) of TiO_2 and RuO_2 are a measure of this property. Since the deposition is initiated through ion exchange followed by the surface fixation of the nuclei in hydrolyzed form at a pH close to their isoelectric point, the depositing nuclei prefer a surface with favorable energy. The adherence of the nuclei to the support particle will be further strengthened in a domain where they have opposite surface charges. Since the preparation procedure involves an acid–base neutralization step, surface thermodynamic properties such as heat of neutralization of the solid surface also have a role to play (*38*). The isoelectric point of P25 TiO_2 is pH 5.8 (*39*). In the presence of Cl^- this is expected to be around pH 6.4 (*39, 40*). The iep of RuO_2 in the presence of Cl^- is around 5.7 pH units (*41*). However, it varies with the preparation procedures and surface treatments (*41*). During the precipitation stage, instead of RuO_2 we have $Ru(OH)_3$ and the iep of this species is expected to be different from that of RuO_2. Therefore it is reasonable to believe that in the pH region 4 to 6, TiO_2 would have positive surface charge and RuO_2 negative charge. Therefore a catalyst prepared at a final pH of 4–6 has the possibility of maximum adherence of one species over the other. Near the point of zero charge any small difference in surface energy between rutile and anatase would influence the stability of fixation of incoming nascent nuclei or particles. Recently, Subramaniam *et al.* (*42*) have clearly shown, using TiO_2–Al_2O_3 composite as an example, that it is possible to direct the ion exchange preferentially to a specific component of the oxide system if for this component the iep is known.

4.2. Reactions of CO

Since there are several routes available for CO conversion to CO_2 and NO to N_2O and their individual elements, elucidating an exact reaction mechanism is extremely useful though very difficult. This aspect is further complicated by the fact that the chemisorption stoichiometry of both CO and NO is a variable because the proportion of linear to bridged forms can vary depending on the nature of the catalyst and experimental conditions. In fact, DRIFT spectroscopy measurements on this catalyst (*31*) have shown that both forms of CO can exist together on the catalyst surface. That is why we have chosen to keep at least a minimum of two monolayers of CO in our CO disproportionation experiments after the catalyst is treated in a vacuum. An excess of CO is thus maintained like a reservoir during the initial stages of the reaction. This could eliminate the strong influence of a particular type of adsorbed CO on the Boudouard reaction. A pool of excess CO could replenish the highly reactive species during the initial stages of the reaction as and when it is reacted to CO_2. After the reaction we find that some of the Ru-loaded TiO_2 crystallites are covered with a thin layer of light material (Fig. 15a). In other areas such surfaces are clean (Fig. 15b). From the history of the catalyst sample and from the CH_4 evolution experiment carried after evacuation, we can conclude that this thin layer is the carbon formed during the Boudouard reaction. Similar conclusions have been arrived at by Kobori *et al.* (*43*) using ^{13}C-labeled CO over Ru supported on SiO_2 at 140°C. Low-temperature CO disproportionation has been intensively studied on Ru single crystal samples as well (*44*). Further work is necessary to answer this question in a detailed way.

Of all the metals studied, Ru and Rh are known to adsorb CO in a nondissociative way at ambient temperatures (*45*). At temperatures around 200°C, they adsorb dissociatively. On the other hand, Cu adsorbs CO nondissociatively even at 200–300°C (*45*). However, the chemisorption stoichiometry of CO on these metals may vary widely. For example, when Ru has one

CO adsorbed per Ru, Rh can have a ratio of CO to Rh up to 2:1 depending on the loading level of Rh and the nature of the support (*12*).

On a partially oxidized Ru particle here termed as Ru–RuO_x, a dipole M^+–O^- is expected. When CO is nondissociatively chemisorbed on such a surface, the C–O bond weakens by back donation of electrons, metal → CO. Consequently, E (1π) increases more than E (4σ) and Δ ($1\pi - 4\sigma$) increases with back bonding. The average value of Δ for Ru is 3.15 eV (*45*). Therefore adsorbed CO can react with another CO even at low temperatures to form CO_2, leaving behind C on the metal. CO disproportionation at room temperature is therefore rationalized. In a flow-through system at low temperatures, this may not be a prominent enough step to be detected because of the small contact time and low reaction rates. Alternatively, adsorbed CO takes up an oxygen from RuO_x to desorb as CO_2. In the presence of NO or H_2O, CO oxidation is facilitated.

4.3. CO + NO Reaction

The reaction of CO with NO over Rh/SiO_2 catalysts has been shown to be a structure-sensitive reaction (*46*). From our results the obvious difference between Ru and Rh catalysts is that whereas Ru favors the formation of more gas-phase N_2O, with Rh a better reduction of NO to individual elements results. Of several studies on NO decomposition over Rh catalysts (*7, 8, 10, 12, 24, 47* and references therein) only a few have identified N_2O as one of the products (*8, 10, 24*). The controversy regarding N_2O formation during NO + CO reaction on Rh catalysts has been addressed recently by Cho *et al.* and others (*8, 47*). They have shown that N_2O is indeed an intermediate in CO + NO and NO decomposition reaction. This was more evident when the catalyst temperatures were low and/or NO concentration relatively high (*10, 47*). When Arai and Tominaga (*48*) investigated the IR absorption bands of CO–NO adsorption over Rh catalysts, only a weak band that disappears on heating at 2225 cm^{-1} (attributed to N_2O(a)) was noted. This was noted only when NO was first preadsorbed before admitting CO. According to Brodén's (*45*) classification Ru adsorbs NO dissociatively whereas Rh is borderline between nondissociative and dissociative adsorption. Several studies have indicated that NO adsorbs on Rh molecularly with a high sticking probability (*12* and references therein). At elevated temperatures, adsorbed NO undergoes extensive dissociation. Hecker and Bell (*24*) have shown that when NO conversion is less than 50%, the kinetic parameters and activation energy values of NO reduction and N_2O/N_2 formation are very similar.

In the present study, the catalyst surface is only partially reduced, whereas Ru exists in different oxidation states, from Ru(0) to Ru(IV). The reaction mechanism may follow any or all of the following stages: (i) through N_2O intermediacy, (ii) through NO decomposition directly to N_2 and $\frac{1}{2}O_2$ on the catalyst surface, and (iii) through an intermediate involving nitrogen, carbon, and oxygen. When NO was passed over the catalyst without CO, both N_2 and N_2O were observed in the product stream and the conversion was independent of reaction temperature. Therefore the additional N_2O and N_2 produced with increasing temperature during NO + CO reaction must be coming from a mechanism involving a different intermediate. Such an intermediate could be an isocyanate species similar to that proposed by Unland (*48, 49*). The reaction mechanism therefore can be proposed as

$$NO \rightarrow NO_{(a)} \quad (4)$$

$$NO_{(a)} \rightarrow N_{(a)} + O_{(a)} \quad (5)$$

$$NO_{(a)} + N_{(a)} \rightarrow N_2O_{(a)} \quad (6)$$

$$N_2O_{(a)} \rightarrow N_2O_{(g)} \quad (7)$$

$$N_2O_{(a)} \rightarrow N_2 + O_{(a)} \quad (8)$$

$$2N_{(a)} \rightarrow N_{2(g)}. \quad (9)$$

Reactions (4) to (9) are independent of reaction temperature. $O_{(a)}$ may also react with NO to form NO_2, which would further react

quickly. A sum of the reaction steps can be written as

$$4NO \rightarrow N_2 + N_2O + \tfrac{3}{2}O_2. \quad (10)$$

When CO is present along with NO,

$$CO_{(g)} \rightarrow CO_{(a)} \quad (11)$$

$$CO_{(a)} + O_{(a)} \rightarrow CO_{2(a)} \rightarrow CO_{2(g)} \quad (12)$$

$$CO_{(a)} + N_2O_{(a)} \rightarrow CO_{2(a)} + N2_{(a)} \rightarrow CO_{2(g)} + N_{2(g)} \quad (13)$$

$$CO_{(a)} + NO_{(a)} \rightarrow CO_2 + N_{(a)} \quad (14)$$

Therefore $CO_{(a)}$, other than its reaction with $NO_{(a)}$, also scavenges $N_2O_{(a)}$ as well as $O_{(a)}$ faster. It is possible that the rate of $CO_{(a)} + O_{(a)}$ reaction is faster than that of CO + N_2O since it took 8 h to react completely 1 ml CO and 370 μl N_2O. On the other hand, it took only <3 h to consume 1 ml CO in NO–CO reaction where CO can react per Eqs. (12), (13), and (14). In such experiments N_2O remained in the cell for a longer time than CO. In the initial stages of the experiment in a batch reactor there is a N_2O buildup period (Figs. 7, 14). This was observed for both light and thermally activated cases. When present, CO accelerated total NO reduction by scavenging $O_{(a)}$ formed in Eq. (5). Equation (6) follows with the formation of N_2O. Several studies (*8*, *12*) have shown that NO dissociation has a relatively large activation barrier and proceeds via a route involving a vacant neighbor site. When the available CO is oxidized to CO_2 completely and the remaining N_2O is slow to decompose according to Eq. (8) with an additional injection of CO, the N_2O reduction was complete in a short time. This shows that step (13) is faster than step (8). N_2O and CO have been shown also to react very well over Rh/Al_2O_3 catalysts (*47*).

Further, CO is oxidized by other sequences such as Eqs. (3) and (15).

$$CO + O(\text{catalyst}) \rightarrow CO_2. \quad (15)$$

Reaction (3) is not a major pathway when NO, N_2O, or H_2O is present.

4.4. Role of Light

It is clear from our data (Figs. 6–9) that on TiO_2-supported catalysts, the complete disappearance of N_2 originating from CO–NO reaction is light sensitive. (The role of light in the formation of N_2O is not so clear.) In dark N_2O remains in the cell even after 25 h (Figs. 7 and 8). Similarly, over Al_2O_3- and SiO_2-supported catalysts the N_2O remained unreacted in the cell at the end of the reaction. The formation of N_2O proceeds via "Metal-N" (i.e., $N_{(a)}$), described by Eq. (6). The same adsorbed species has been shown to be responsible for the formation of –NCO as an intermediate (*48*, *49*). In our case N_2O and –NCO formation is facile since the system is not in a net oxidizing environment: the catalyst was prereduced and there was no added O_2. Hecker and Bell (*50*) have shown by IR spectroscopy that –NCO species formed on the metal site readily migrate onto the support. Scheme 1 presents a possible path of NO–CO reaction at low temperature with some of the steps support related. Such support-related sequences have an additional possibility of becoming activated by light absorption. When the reaction is thermally activated (i.e., in the absence of light irradiation), –NCO species is known to not take part in the actual reaction mechanism (*47*, *50*, *51*). The sequences in Scheme 1 are based on the fact that NO is adsorbed more strongly than CO (*24*). Cho *et al.* (*47*) have recently reported that reactions (16) and (17) are important at low temperatures, while reaction (18) becomes important at high temperatures.

$$2NO + CO \rightarrow N_2O + CO_2 \quad (16)$$

$$N_2O + CO \rightarrow N_2 + CO_2 \quad (17)$$

$$NO + CO \rightarrow \tfrac{1}{2}N_2 + CO_2. \quad (18)$$

We propose that these low-temperature reactions are prone to activation by light and further work is in progress to check this aspect.

The photoactive support under illumination can activate –NCO and replenish that

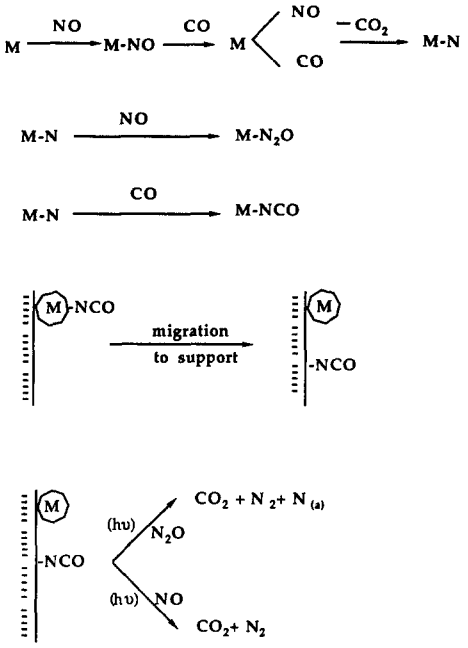

SCHEME 1. The hν indicates that the reaction is also facilitated by light of proper λ. M represents catalytically active metal particle attached to the support.

site for further –NCO migration, leading to faster NO reduction. Since M–N can lead to –NCO and N_2O formation, a faster rate through the –NCO route means less amounts of N_2O in the system. On the other hand, N_2O also is reduced on Ru/TiO_2 faster under light (Fig. 6–8) owing to photogenerated electron transfer from TiO_2 to $Ru–RuO_x$. These processes do not proceed well on a support such as SiO_2 and Al_2O_3. It is possible that Ti–NCO is participating in the catalytic process, unlike Si–NCO which is very stable and inert in the NO reduction process as observed by Hecker and Bell (*50*). On Al_2O_3 there is evidence for surface-state initiated photoprocesses (*34, 35*) leading to mild photoresponses. Indeed, it is reflected on our results (Fig. 11). Therefore we can conclude that the photoprocesses are basically support related.

4.5. Influence of Rh and Cu

When Rh was present along with Ru, the amount of N_2O that appeared in the gas phase was relatively small (Fig. 14) and the total reduction of NO to N_2 was higher, indicating the increased activity of added Rh for the reaction. CuO_x also accelerated this reaction, but not to the level of Rh. The patterns of activity by Cu and Rh catalysts are similar. The appearance of N_2O on Rh/TiO_2 catalysts is an important observation because there are few other reports on the formation of gas-phase N_2O over Rh catalysts (*8, 10, 47*). Chin and Bell (*8*) noted that at room temperature about 9% NO remains adsorbed dissociatively and upon heating it was released as $N_{2(g)}$ and $O_{2(g)}$. A small amount of N_2O was also formed. Hecker and Bell (*24*) have shown that preoxidation of the catalyst (Rh/SiO_2) results in a 50% higher NO reduction activity with about 5% lower N_2O selectivity than when the catalyst is prereduced. In all our experiments we used a large partial pressure of NO at low temperatures over a prereduced catalyst. It should be stressed that NO–CO reaction is structure sensitive (*46*) and hence the type of catalyst used is important. Rh surfaces are known to be predominantly covered with adsorbed NO (*51*) and the formation of N_2O is related to the presence of molecularly adsorbed NO. Previous studies (*24*) on Rh/SiO_2 have shown that at temperature above 190°C, N_2O once formed does not undergo further reduction even in the presence of CO. This was not true in our case, suggesting that the low-temperature mechanism for CO–NO reaction with a possible involvement of the support is different from that at high temperature on metal-loaded inert supports. Niwa *et al.* (*52*) have reported that CeO_2 and SnO_2 could adsorb NO dissociatively to form N_2 and N_2O. TiO_2, another four-valent metal oxide of similar properties, may have the same quality.

5. CONCLUSION

The present study has initiated a new route for low-temperature NO–CO reaction. One of the catalysts, Ru supported on TiO_2, shows interesting surface morphology. This is exhibited by a selective deposi-

tion of Ru particles on the rutile phase of P25. Photothermal activation was shown to be possible over such catalysts at ambient temperature. Addition of Rh and Cu has beneficial effects on the reduction of N_2O, a by-product of the reaction. The mechanism of thermal activation has been widely studied and this study suggests that all aspects of that mechanism may not be valid for the photoprocess. The reaction mechanism depicted in Scheme 1 is in accordance with our experimental findings and those of others found in the literature. This scheme proposes possible steps whereby light can beneficially influence the reaction sequence. A thorough study is needed to understand the photomechanism. Based on the experience from this study, it is our aim to develop catalysts which are "bifunctional," such as WO_3–TiO_2, V_2O_3–TiO_2, and Pt–WO_3–TiO_2. Such catalysts can absorb both UV and visible regions of the spectrum. Regalbuto and Wolf have shown that NO–CO reaction over Pt/SiO_2 catalysts is promoted by WO_3 (*53*). Therefore, in principle, WO_3 should promote the reaction in a bifunctional mode. Under thermal activation it acts as a promoter, but under simultaneous light irradiation it could also enhance the reaction rate by light absorption.

ACKNOWLEDGMENTS

Financial support from Gas Research Institute, Chicago, (subcontract through SERI, Golden, Colorado) is gratefully acknowledged.

REFERENCES

1. Jansen, F. J. J. G., and Van den Kerkhof, F. M. G., *in* "Kema Scientific and Technical Reports," Vol. 3, No. 6. N. V. Kema, Arnheim, Holland, 1985.
2. Bosch, H., and Janssen, F., *Catal. Today* **2,** 369 (1988).
3. McEvoy, A. J., Revilliod, C., Thampi, K. R., and Grätzel, M., *in* "Proc. 4th Int. Symp. Res. Dev. and Appl. of Solar Thermal Technol., 1988, Santa Fe." Hemisphere Publishing Co., New York, 1990.
4. Lyashenko and Gorokhovat-skii, Y. B., *Theor. Exp. Chem. Engl. Transl.*, **10,** 138 (1975).
5. Chen, B. H., Close, J. S., and White, J. M., *J. Catal.* **46,** 253 (1977).
6. Koel, B. E., White, J. M., Erskine, J. L., and Antoniewicz, *in* "Interfacial Photoprocesses: Energy Conversion and synthesis" (M. S. Wrighton, Ed.), Adv. in Chem. series 184. Amer. Chem. Soc., Washington D.C., 1980.
7. Kobylinski, T. P., and Taylor, B. W., *in* "Proc. of Divn. of Petrol. Chem. meeting," p. 431. Amer. Chem. Soc., Washington D.C., 1973.
8. Chin, A. A., and Bell, A. T., *J. Phys. Chem.* **87,** 3700 (1983).
9. Kummer, J. T., *J. Phys. Chem.* **90,** 4747 (1986).
10. Hardee, J. R., and Hightower, J. W., *J. Catal.* **86,** 137 (1984).
11. Wickham, D. T., and Koel, B. E., *J. Catal.* **114,** 207 (1988).
12. Oh, S. H., Fisher, G. B., Carpenter, J. E., and Goodman, D. W., *J. Catal.* **100,** 360 (1986).
13. Bosch-Driebergen, A. G., Kieboom, M. N. H., Dreumel, A., Wolf, R. M., Delft, F. C. M. J. M., and Nieuwenhuys, B. E., *Catal. Lett.* **2,** 235 (1989).
14. Taylor, K. C., *in* "Catalysis Science and Technology" (J. R. Anderson and M. Boudart, Eds.), Vol. 5, p. 119. Springer-Verlag, Berlin, 1984.
15. Mizuno, N., Fujiwara, Y., and Misono, M., *J. Chem. Soc., Chem. Commun.*, 316 (1989).
16. Bhaduri, S., and Johnson, B. F. G., *Transition Met. Chem.* **3,** 156 (1978).
17. Kubota, M., Evans, K. J., Koerntgen, C. A., and Marsters Jr., J. C., *J. Amer. Chem. Soc.* **100,** 342 (1978).
18. Goodman, D. W., and Peden, C. H. F., *J. Phys. Chem.* **90,** 4839 (1986).
19. Thampi, K. R., Kiwi, J., and Grätzel, M., *Nature (London)* **327,** 506 (1987).
20. Thampi, K. R., Kiwi, J., and Grätzel, M., *in* "Proc. 9th Int. Congr. on Catalysis" (M. J. Phillips and M. Ternan, Eds.), Vol. 2, p. 837. Chemical Institute of Canada, Ottawa, 1988.
21. Kobylinski, T. P., and Taylor, B. W., *J. Catal.* **33,** 376 (1974).
22. Butler, J. D., Davis, D. R., *J. Chem. Soc. Dalton Trans.*, 2253 (1976).
23. Shelef. M., Otto. M., and Gandhi, H., *J. Catal.* **12,** 361 (1968).
24. Hecker, W. C., and Bell, A. T., *J. Catal.* **84,** 200 (1983).
25. Hugo, P., *in* "Proc. 4th European symposium on Chem. React. Eng., Brussels," p. 459, 1968.
26. Bauerle, G. L., Service, G. R., and Nobe, K., *Ind. Eng. Chem. Prod. Res. Dev.* **11,** 54 (1972).
27. Ramanujachary, K. V., and Swamy, C. S., *in* "Proc. 5th National Catal. Symp. (India)," p. 84. Catal. Soc. India, 1983.
28. Gunasekaran, N., Meenakshisundaram, A., and Srinivasan, V., *Indian J. Chem. Sect. A* **21,** 346 (1982).
29. Groeneveld, M. J., Boxhoorn, G., Kuipers, H. P. C. E., van Grinsven, P. F. A., Gierman, R., and Zuideveld, P. L., *in* "Proc. 9th Int. Cong.

Catal." (M. J. Phillips and M. Terman, Eds.), Vol. 4, p. 1743. Chemical Inst. Canada, Ottawa, 1988.
30. Prairie, M. R., Highfield, J. G., and Renken, A., *Chem. Eng. Sci.*, in press.
31. Prairie, M. R., Renken, A., Highfield, J. G., Thampi, K. R., and Grätzel, M., in preparation.
32. Ruterana, P., Buffat, P-A., Thampi, K. R., and Grätzel, M., *Mater. Res. Soc. Symp. Proc.* **139,** 327 (1989).
33. Fabel, G. W., Cox, S. M., and Lichtman, D., *Surf. Sci.* **40,** 571 (1973).
34. Mansour, A., Balard, H., Papirer, E., *J. Chem. Phys.* **84,** 569 (1987).
35. Grätzel, M., Thampi, K. R., and Kiwi, J., *J. Phys. Chem.* **93,** 4128 (1989).
36. Highfield, J. G., Ruterana, P., Thampi, K. R., and Grätzel, M., *in* "Structure and Reactivity of Surfaces" (C. Morterra, A. Zecchina, and G. Costa, Eds.), p. 469. Elsevier, Amsterdam, 1989.
37. James, R. O., and Parks, G. A., *Surf. Colloid Sci.* **12,** 119 (1982).
38. Hunter, R. J., *in* "Zeta Potential in Colloid Science," Chap. 6. Academic Press, London, 1981.
39. Degussa Bulletin (number 56). Degussa GmbH, West Germany.
40. Parks, G. A., *Chem. Rev.* **65,** 177 (1965).
41. Ardizzone, S., Siviglia, P., and Trasatti, S., *J. Electroanal. Chem.* **122,** 395 (1981).
42. Subramanian, S., Noh, J. S., and Schwarz, J. A., *J. Catal.* **114,** 433 (1988).
43. Kobori, Y., Yamasaki, H., Naito, S., Onishi, T., and Tamaru, K., *J. Chem. Soc. Faraday Trans. 1* **78,** 1473 (1982).
44. Shincho, E., Egawa, C., Naito, S., and Tamaru, K., *Surf. Sci.* **155,** 153 (1985).
45. Brodén, G., Rhodin, T. N., Brucker, C., Benbow, R., and Hurych, Z., *Surf. Sci.* **59,** 593 (1976).
46. Hecker, W. C., and Breneman, R. B., *in* "Catalysis and Automotive Pollution Control" (A. Crucq and A. Frennet, Eds.), p. 257. Elsevier, Amsterdam, 1987.
47. Cho, B. K., Shanks, B. H., and Bailey, J. E., *J. Catal.* **115,** 486 (1989) and references therein.
48. Arai, H., and Tominaga, H., *J. Catal.* **43,** 131 (1976).
49. Unland, M. L., *J. Catal.* **31,** 459 (1973); *J. Phys. Chem.* **77,** 1952 (1973).
50. Hecker, W. C., and Bell, A. T., *J. Catal.* **85,** 389 (1984).
51. Oh, S. H., and Carpenter, J. E., *J. Catal.* **101,** 114 (1986).
52. Niwa, M., Furukawa, Y., and Murakami, Y., *J. Colloid Interface Sci.* **86,** 260 (1982).
53. Regalbuto, J. R., and Wolf, E. E., *in* "Catalysis and Automotive Pollution Control" (A. Crucq and A. Frennet, Eds.), p. 345. Elsevier, Amsterdam, 1987.